Journal of Alloys and Compounds 502 (2010) 456–460

Contents lists available at ScienceDirect

Journal of Alloys and Compounds

journal homepage: www.elsevier.com/locate/jallcom

The Ag effect on magnetic properties and microstructure of FePt/Ag_2Te particulate films

Jai-Lin Tsai*, Hsin-Te Tzeng, Guo-Bing Lin, Bing-Fong Liu

Department of Materials Science and Engineering, National Chung Hsing University, 250 Kuo Kuang Rd., Taichung 402, Taiwan

ARTICLE INFO

Article history:
Received 23 March 2010
Received in revised form 19 April 2010
Accepted 25 April 2010
Available online 5 May 2010

Keywords:
Particulate film
Perpendicular magnetization

ABSTRACT

A [FePt (1 nm)/$Ag_2Te(t)]_{10}$ (thickness t = 0.1–0.3 nm) multilayer was deposited alternately on glass substrate and subsequently annealed by a rapid thermal process (RTP). After the RTP, the interface between FePt and Ag_2Te was intermixed, forming particulate films. The $L1_0$ FePt grain size decreases from 23 to 14 nm as t of the Ag_2Te intermediate layer increases from 0.1 to 0.3 nm. The $(FePt/Ag_2Te)_{10}$ particulate film shows perpendicular magnetization. Compared to $(FePt/Ag_2Te)_{10}$, the Ag/$(FePt/Ag_2Te)_{10}$/Ag multilayer also shows perpendicular magnetization with less c-axis dispersion. The Ag capping and seed layers reduce the ordering temperature of FePt but facilitate its grain growth during RTP. As a result, the FePt grains are refined and well-separated by the Ag_2Te phase, but change to a continuous film after inserting Ag capping and seed layers.

1. Introduction

(0 0 1) textured $L1_0$ FePt thin film has high magnetocrystalline anisotropy field and good corrosion resistance, which are required for hard magnetic materials and for high-density magnetic recording media. Due to its high uniaxial anisotropy, the super-paramagnetic limit was extended and thermal stability was achieved, even when the grain size of FePt was reduced to 5 nm [1–4]. Granular type magnetic recording media was used conventionally, however, maintaining the signal to noise ratio with increasing recording density requires magnetic media with smaller grain size. This decrease in grain size and exchange coupling are usually achieved by adding materials, such as amorphous MgO, B_2O_3, SiO_2, Al_2O_3, and AlN into FePt film or a Fe/Pt multilayer and forming the granular structure after annealing. $L1_0$ FePt film with perpendicular magnetization was prepared by creating an appropriate epitaxial buffer layer on a single crystal substrate [5–7], or by forming the c-axis texture on an amorphous substrate [8–10]. FePt films with a thin Ag layer have been discussed extensively, due to the immiscibility of FePt and Ag [11–13]. (0 0 1) textured FePt:TiO_2, $(Fe/Pt/SiO_2)_x$ nanocomposite films, composed of isolated 5 nm grains of FePt have been reported [14,15]. In our previous work, the Ag/FePt bilayer and Ag/FePt/Ag trilayer annealed by a rapid thermal process (RTP) at 800 °C are continuous films with perpendicular magnetization [16]. Ag has a high thermal diffusivity that reduces the ordering temperature of FePt, yet enhances grain growth during RTP. In this study, we compared the magnetic properties and microstructure of multilayer $(FePt/Ag_2Te)_{10}$, and Ag/$(FePt/Ag_2Te)_{10}$/Ag. The intermetallic compound Ag_2Te has a low melting point (960 °C) almost equal to that of Ag (962 °C). Metallic Ag has limited solubility (~6.9%) in $L1_0$ FePt that is not suitable for isolation of FePt grains at a high annealing temperature. The Ag_2Te compound has a covalent/ionic character with higher resistivity [$1–4 \times 10^{-3}\ \Omega$ m] than metallic Ag [$1.587 \times 10^{-8}\ \Omega$ m]. The bonding characteristic of Ag_2Te is similar to that of SiO_2, TiO_2, and MgO, and better for the FePt matrix than Ag. The Ag_2Te is also a thermoelectric material with low thermal conductivity and a high-power factor, which is defined as the square of the Seebeck coefficient times the electrical conductivity [17].

2. Experimental

The multilayers [FePt (1 nm)/$Ag_2Te(t)]_{10}$ (thickness t = 0.1–0.3 nm), Ag (1 nm)/[FePt (1 nm)/$Ag_2Te(t)]_{10}$/Ag (0.1 nm) were fabricated by DC magnetron sputtering. The base pressure of the sputtering system was 5×10^{-8} Torr and the working pressure was 1.5×10^{-3} Torr under high purity argon gas. FePt, Ag_2Te, and Ag targets were used, and the films were deposited on a glass substrate. After deposition, the films were annealed by a rapid thermal annealing (RTA) system at 800 °C for 10 min. The heating rate in RTA is 10 °C/s much higher than in a traditional furnace. The crystal structure of samples was identified by grazing incident X-ray diffractometry (XRD) with Cu Kα radiation. The microstructure of the films was observed by high resolution transmission electron microscopy (HRTEM). Magnetic hysteresis loops were measured at room temperature using a vibration sample magnetometer (VSM) with a maximum magnetic field of 2 T.

3. Results and discussion

Fig. 1 shows XRD patterns of the single-layer FePt, multilayer [FePt/Ag_2Te $(t)]_{10}$ (t = 0.1, 0.3, and 0.4 nm, respectively), trilayer

* Corresponding author. Tel.: +886 4 22875741; fax: +886 4 22857017.
E-mail address: tsaijl@dragon.nchu.edu.tw (J.-L. Tsai).

0925-8388/$ – see front matter © 2010 Elsevier B.V. All rights reserved.
doi:10.1016/j.jallcom.2010.04.195

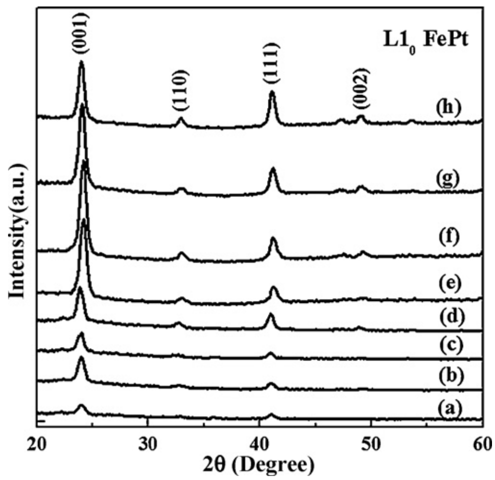

Fig. 1. XRD patterns of films annealed at 800 °C for 10 min: (a) FePt single layer, (b) [FePt/$Ag_2Te(t)]_{10}$ multilayers, t = 0.1 nm, (c) t = 0.3 nm, (d) t = 0.4 nm; (e) Ag/FePt/Ag trilayer, (f) Ag/[FePt/$Ag_2Te(t)]_{10}$/Ag multilayer, t = 0.1 nm, (g) t = 0.3 nm, (h) t = 0.4 nm.

Ag/FePt/Ag and multilayer Ag/[FePt/Ag_2Te $(t)]_{10}$/Ag annealed at 800 °C for 10 min. For the FePt single layer and Ag/FePt/Ag trilayer shown in Fig. 1(a) and (e), the film showed preferential orientation in the [0 0 1] direction. The relative intensity of the fundamental peak (1 1 1) is low. The XRD patterns of the multilayers [FePt/$Ag_2Te(t)]_{10}$ and Ag/[FePt (1 nm)/$Ag_2Te(t)]_{10}$/Ag (t = 0.1, 0.3, and 0.4 nm, respectively) are plotted in Fig. 1(b–d) and (f–h), respectively. The superlattice diffraction peak (0 0 1) dominates and the low intensity of the (1 1 1) peak is also indexed. When t = 0.4 nm, the relative intensity of the (1 1 1) peak is increased to half that of the (0 0 1) peak, indicating that FePt grains are tend to orient isotropically. In summary, the FePt (0 0 1) orientation is deteriorated by inserting an Ag_2Te layer, but is still dominant in the multilayers.

The semi-quantitative method, the Lotgering orientation factor (LOF), was used to analyze the variation of the (0 0 1) preferred orientation. The LOF represents the degree of specific texture and has values ranging from 0 to 1, where 0 and 1 indicate a random distribution and perfect crystal orientation, respectively. When the specific orientation is {0 0 1}, the LOF is defined as follows [19]:

$$\mathrm{LOF} = \frac{P - P_0}{1 - P_0}$$

$$\text{where } P = \frac{\sum (0\,0\,1)_{\text{sample}}}{\sum (h\,k\,l)_{\text{sample}}}, \quad P_0 = \frac{\sum (0\,0\,1)_{\text{powder}}}{\sum (h\,k\,l)_{\text{powder}}} \tag{1}$$

For the calculation of sample orientation, the P value was estimated from the intensity summation of the {0 0 l} orientation over the intensity summation of ($h\,k\,l$) reflections ranging from 20 to 80°. For the non-oriented sample (P_0 value), the simulation data was used to replace the free textured FePt powder sample. Table 1 lists the LOF values of a single-layer FePt, multilayer [FePt/Ag_2Te $(t)]_{10}$ (t = 0.1, 0.3, and 0.4 nm, respectively), trilayer Ag/FePt/Ag, and multilayer Ag/[FePt/Ag_2Te $(t)]_{10}$/Ag annealed at 800 °C for 10 min. The trilayer Ag/FePt/Ag (0.73) has a higher LOF value than single-layer FePt (0.49). For the multilayers [FePt/Ag_2Te $(t)]_{10}$, Ag/[FePt/Ag_2Te $(t)]_{10}$/Ag (t = 0.1 and 0.3 nm, respectively), the similar LOF values are 0.69, 0.65 and 0.70, 0.63, respectively. However, the in-plane magnetic hysteresis loops are more linear in the multilayer Ag/[FePt/Ag_2Te $(t)]_{10}$/Ag (t = 0.1, 0.3) shown in Fig. 3(e) and (f). When the thickness of the Ag_2Te layer reaches 0.4 nm per pair in the multilayer [FePt/Ag_2Te $(t)]_{10}$, Ag/[FePt/Ag_2Te $(t)]_{10}$/Ag, the LOF values decrease to 0.49 and 0.39, respectively.

Table 1
The LOF, FWHM, and (0 0 1) peak values of a single-layer FePt, multilayer [FePt/Ag_2Te $(t)]_{10}$ (t = 0.1, 0.3 and 0.4 nm, respectively), trilayer Ag/FePt/Ag and multilayer Ag/[FePt/Ag_2Te $(t)]_{10}$/Ag annealed at 800 °C for 10 min.

XRD	2θ (0 0 1)	Δθ	FWHM	LOF
(a) FePt single layer	23.99	–	0.63	0.49
(b) (FePt/Ag_2Te (0.1 nm))$_{10}$	23.98	–	0.56	0.69
(c) (FePt/Ag_2Te (0.3 nm))$_{10}$	23.91	–	0.58	0.65
(d) (FePt/Ag_2Te (0.4 nm))$_{10}$	23.89	–	0.54	0.49
(e) Ag/FePt/Ag trilayer	24.16	(e)–(a) 0.17	0.58	0.73
(f) Ag/(FePt/Ag_2Te (0.1 nm))$_{10}$/Ag	24.15	(f)–(b) 0.17	0.58	0.70
(g) Ag/(FePt/Ag_2Te (0.3 nm))$_{10}$/Ag	24.15	(g)–(c) 0.24	0.57	0.63
(h) Ag/(FePt/Ag_2Te (0.4 nm))$_{10}$/Ag	24.16	(h)–(d) 0.27	0.53	0.40

The ordering degree S is not easy to estimate by lattice constants c (c-axis spacing) over a (a-axis spacing), c/a ratio, from the (0 0 1) and (1 1 0) peaks or from the intensity ratio of the (0 0 1) and (0 0 2) peaks ($I_{(001)}/I_{(002)}$) due to the weak diffraction peaks of (1 1 0), and (0 0 2). In Table 1, for the same thickness of the inserted Ag_2Te layer, the (0 0 1) peak shifts to higher angles, as evident from Fig. 1(e)–(a), Fig. 1(f)–(b), Fig. 1(g)–(c), and Fig. 1(h)–(d), respectively, indicating that the lattice constant c is decreased. The ordering of the multilayer Ag/[FePt/$Ag_2Te(t)]_{10}$/Ag is better than that of [FePt/$Ag_2Te(t)]_{10}$.

The c-axis distribution can be explained more quantitatively by the full width of half maximum (FWHM) variations of the FePt (0 0 1) diffraction peaks and are listed in Table 1. The FWHM values for the multilayers [FePt/Ag_2Te $(t)]_{10}$, Ag/[FePt/Ag_2Te $(t)]_{10}$/Ag (t = 0.4 nm) were discarded because of low LOF values. The c-axis of the trilayer Ag/FePt/Ag (FWHM, 0.58) is less dispersed than that of the single-layer FePt (0.63). For the multilayers [FePt/Ag_2Te $(t)]_{10}$, Ag/[FePt/Ag_2Te $(t)]_{10}$/Ag (t = 0.1 and 0.3 nm, respectively), the similar FWHM values are 0.56, 0.58 and 0.58, 0.57, respectively. The c-axis dispersion of the multilayers is nearly the same.

Fig. 2 shows the magnetic hysteresis loops of single-layer FePt, multilayer [FePt/$Ag_2Te(t)]_{10}$ (t = 0.1 and 0.3 nm, respectively), trilayer Ag/FePt/Ag and multilayer Ag/[FePt/$Ag_2Te(t)]_{10}$/Ag annealed at 800 °C for 10 min. Fig. 2(a) shows the in-plane and out-of-plane hysteresis loops of the FePt single layer annealed at 800 °C and shows that it presents perpendicular magnetization. In Fig. 2(a), the out-of-plane H_c and remanence ratio are 9.8 kOe and 0.93, respectively. The in-plane magnetic hysteresis loop is linear. Fig. 2(b) and (c) show the in-plane and out-of-plane hysteresis loops of the multilayers [FePt/$Ag_2Te(t)]_{10}$ (t = 0.1 and 0.3 nm) annealed at 800 °C. The out-of-plane coercivity and remanence are higher than the in-plane properties for (FePt/Ag_2Te) films. The FePt/Ag_2Te presents perpendicular magnetization with the out-of-plane H_c (10.1 kOe) and remanence ratio (0.84) when the total thickness of Ag_2Te reaches 3 nm (0.3 nm per pair). The high value of in-plane H_c is due to c-axis dispersion but the remanence ratio (M_r/M_s = 0.32) is low. Fig. 2(d) shows in-plane and out-of-plane hysteresis loops of trilayer Ag/FePt/Ag film. The film also shows perpendicular magnetization with the out-of-plane H_c (9.1 kOe) and remanence ratio (0.95). Fig. 2(e) and (f) show the in-plane and out-of-plane hysteresis loops of the multilayers Ag/[FePt/$Ag_2Te(t)]_{10}$/Ag (t = 0.1, 0.3 nm) annealed at 800 °C. In Fig. 2(e) and (f), the films show perpendicular magnetization with higher out-of-plane H_c than seen in multilayer (FePt/Ag_2Te) films. As shown in Fig. 2(e) and (f), the out-of-plane H_c and reamnence ratio are 9.4 and 11.5 kOe, 0.92 and 0.87, respectively. Compared with Fig. 2(b) and (c), the in-plane hysteresis loop is nearly linear.

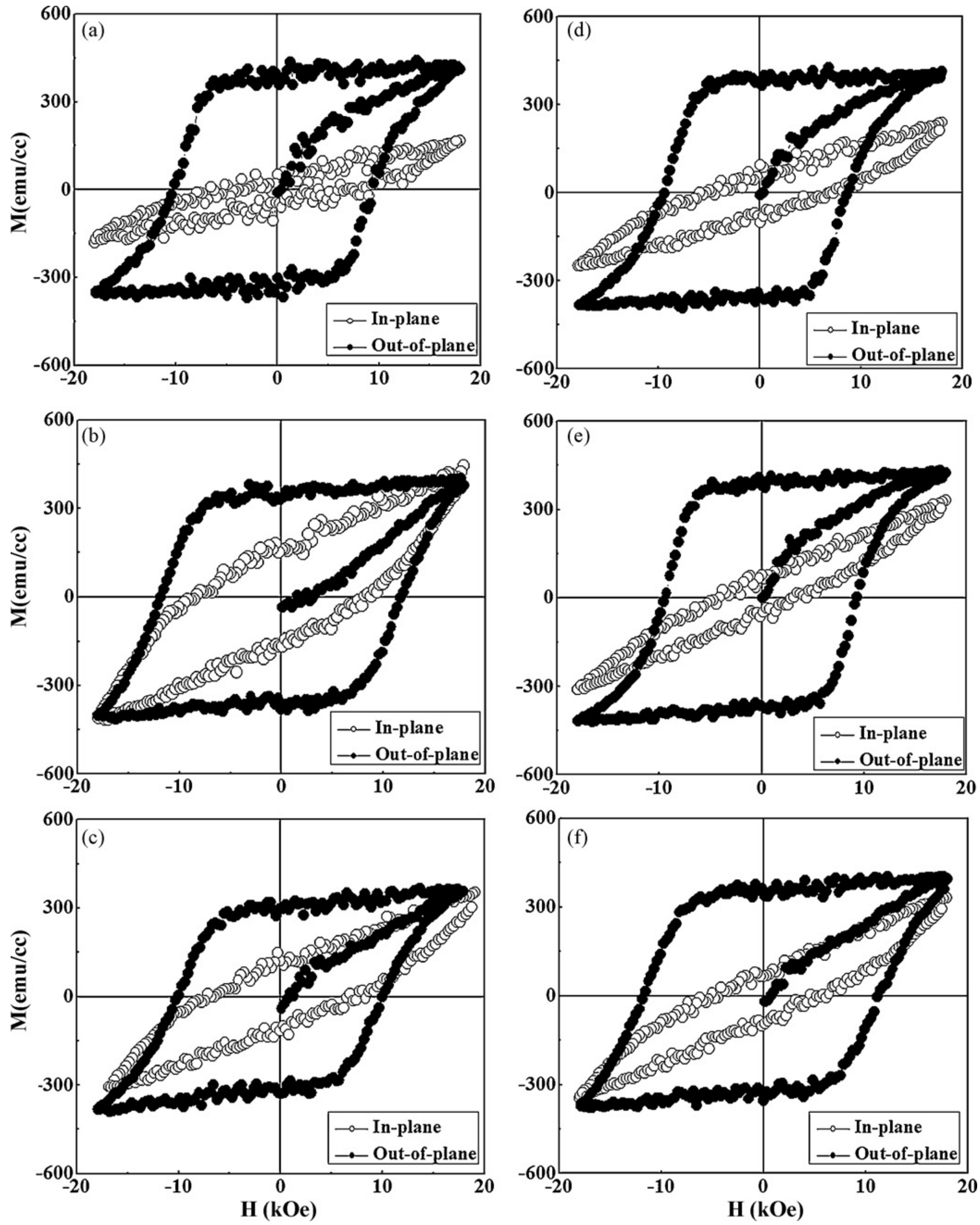

Fig. 2. In-plane and out-of-plane magnetic hysteresis loops of (a) FePt single layer, (b) $[FePt/Ag_2Te(t)]_{10}$ multilayer, $t = 0.1$ nm, (c) $t = 0.3$ nm; (d) Ag/FePt/Ag trilayer, (e) $Ag/[FePt/Ag_2Te(t)]_{10}/Ag$ multilayer, $t = 0.1$ nm, (f) $t = 0.3$ nm.

Fig. 3 shows plane view TEM images and selective area diffraction patterns (SAD) of single-layer FePt, trilayer Ag/FePt/Ag and the multilayers $(FePt/Ag_2Te)_{10}$, $Ag/(FePt/Ag_2Te)_{10}/Ag$, respectively. In Fig. 3(a), the image of FePt film annealed at 800 °C for 10 min shows that the FePt grains are distributed continuously on the glass substrate and the grain size is not uniform. The ring patterns of the (1 1 0), (0 0 2) and (1 1 1) planes were indexed. Fig. 3(b) and (c) show images of the multilayers $(FePt/Ag_2Te(t))_{10}$ ($t = 0.1$ and 0.3 nm) annealed at 800 °C for 10 min. In Fig. 3(b), the FePt grains are separated by 1 nm of Ag_2Te and form a particle-like structure. The FePt grains are round and distributed separately. The twin bands used to release phase transition strains are observed in some FePt grains, and the average grain size is 23 nm. Fig. 3(c) shows TEM images of $[FePt/Ag_2Te\ (0.3\,nm)]_{10}$ film annealed at 800 °C the grains are refined and the average grain size is 14 nm. In summary, the FePt grains are refined and isolated well by the intermetallic compound Ag_2Te layer. Fig. 3(d) shows the image of trilayer Ag/FePt/Ag annealed at 800 °C for 10 min; the FePt grains are distributed nearly continuously with some network structure. Fig. 3(e) and (f) show images of multilayer $Ag/(FePt/Ag_2Te(t))_{10}/Ag$ ($t = 0.1$ and 0.3 nm) annealed at 800 °C for 10 min; the FePt grains are not distributed continuously and present a network structure. In Fig. 3(e) and (f), the FePt grains are located between networks indicated by arrows; the average grains sizes are 11 and 3 nm. According to Pauling's electronegativity, the ionic character (%) = $\{1 - \exp[-(0.25)(X_{Ag} - X_{Te})^2]\} \times 100$, the covalent character of Ag_2Te is 46.1% and ionic character is 53.1% nearly equals to the properties of SiO_2 (51%). The surface energy of glass, Ag_2Te, and FePt are 1.5, 2.1, and 2.8 J/m^2, respectively [9,18]. This result is similar to that the FePt grains in an oxide matrix such as SiO_2, TiO_2 or MgO.

The Wohlfarth relation and Kelly–Henkel plot (δM plot) were used to characterize and classify the hysteresis phenomena, especially the intergrain magnetic interaction. The δM plot can be

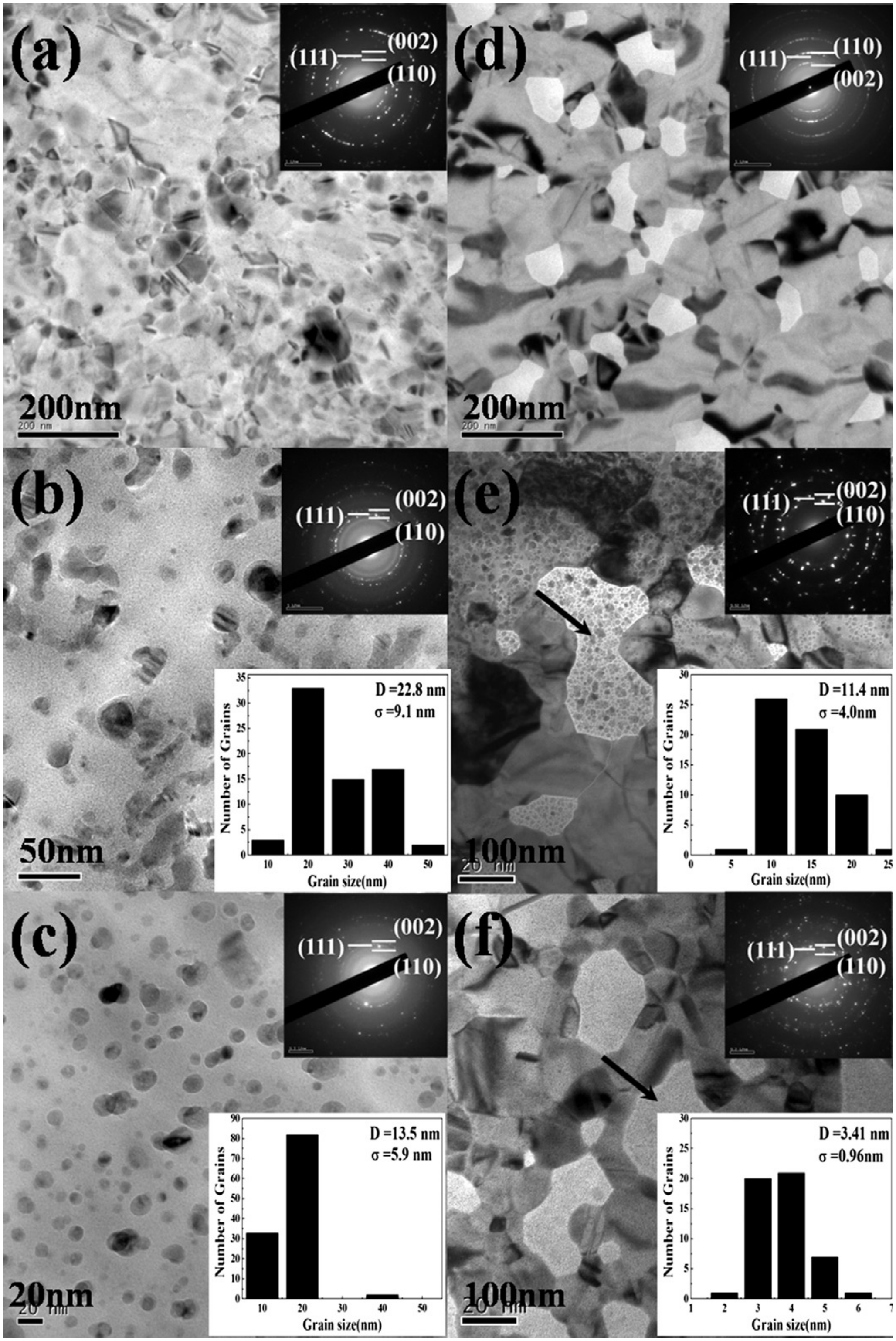

Fig. 3. TEM images of films annealed at 800 °C for 10 min: (a) FePt single layer, (b) $[FePt/Ag_2Te(t)]_{10}$ multilayer, t = 0.1 nm, (c) t = 0.3 nm; (d) Ag/FePt/Ag trilayer, (e) $Ag/[FePt/Ag_2Te(t)]_{10}/Ag$ multilayer, t = 0.1 nm, (f) t = 0.3 nm.

determined from the following equation:

$$\delta M = M_d(H) - [1 - 2M_r(H)] \quad (2)$$

where $M_d(H)$ is the normalized dc-demagnetization(DCD) remanence as a function of the reversal field, and $M_r(H)$ is the normalized isothermal remanence (IRM) curve. From the Kelly–Henkel plot, a positive δM indicates that intergrain interactions are ferromagnetic exchange interactions. A negative δM value suggests that intergrain interactions are dipolar interactions. Fig. 4 shows the δM plots of a FePt single layer, Ag/FePt/Ag trilayer, and multilayers $(FePt/Ag_2Te)_{10}$, $Ag/(FePt/Ag_2Te)_{10}/Ag$. The FePt single layer, Ag/FePt/Ag trilayer, and $Ag/(FePt/Ag_2Te)_{10}/Ag$ multilayer show

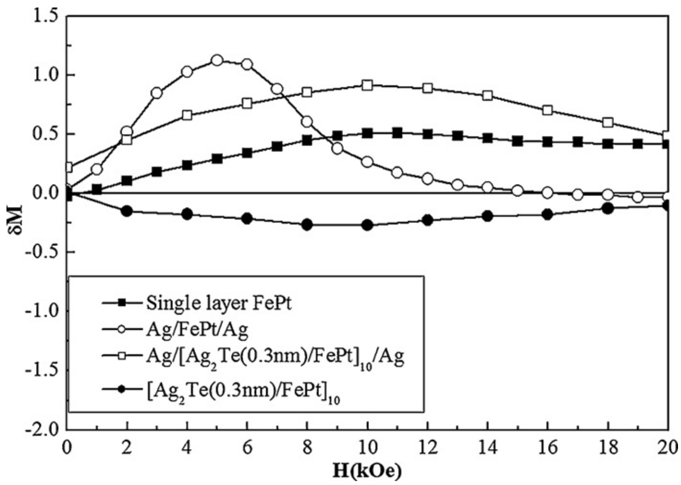

Fig. 4. δM plots of FePt single layer, Ag/FePt/Ag trilayer, multilayers $(FePt/Ag_2Te)_{10}$, $Ag/(FePt/Ag_2Te)_{10}/Ag$.

positive δM values which means a strong intergrain exchange interaction. The $(FePt/Ag_2Te)_{10}$ multilayer without an Ag layer shows a negative δM value at all applied fields. The reduction of exchange interaction between FePt grains was achieved by inserting Ag_2Te inserting layers.

4. Conclusions

In conclusion, FePt film with a perpendicular magnetization was fabricated on a glass substrate and the FePt grains are isolated well by the Ag_2Te phase. The grain size is reduced from hundreds of nanometers in FePt continuous films to 14 nm in particulate [FePt/Ag_2Te (3 nm)] films.

Acknowledgements

The authors would like to thank the NSC of Taiwan for financial support under the grant No. of NSC 97-2221-E-005-022. We also thank the Center of Nanoscience and Nanotechnology in NCHU for the TEM investigation.

References

[1] M.H. Hong, K. Hono, M. Watanabe, J. Appl. Phys. 84 (1998) 4403.
[2] J.P. Liu, C.P. Luo, Y. Liu, D.J. Sellmyer, Appl. Phys. Lett. 27 (1998) 483.
[3] D. Weller, A. Moser, L. Folks, M.E. Best, W. Lee, M.F. Toney, et al., IEEE Trans. Magn. 36 (2000) 10.
[4] T. Shima, K. Takanashi, Y.K. Takahashi, K. Hono, Appl. Phys. Lett. 88 (2006) 063117.
[5] G.R. Trichy, D. Chakraborti, J. Narayan, J.T. Prater, Appl. Phys. Lett. 92 (2008) 102504.
[6] Y. Xu, J.S. Chen, J.P. Wang, Appl. Phys. Lett. 80 (2002) 3325.
[7] C. Feng, Q. Zhan, B. Li, J. Teng, M. Li, Y. Jiang, G. Yu, Appl. Phys. Lett. 93 (2008) 152513.
[8] M.L. Yan, N. Powers, D.J. Sellmyer, J. Appl. Phys. 93 (2003) 8292.
[9] J.S. Kim, Y.M. Koo, B.J. Lee, S.R. Lee, J. Appl. Phys. 99 (2006) 053906.
[10] Y.C. Wu, L.W. Wang, C.H. Lai, Appl. Phys. Lett. 91 (2007) 072502.
[11] Z.L. Zhao, J. Ding, J.B. Yi, J.S. Chen, J.H. Zeng, J.P. Wang, J. Appl. Phys. 97 (10) (2005) H502.
[12] C.Y. You, Y.K. Takahashi, K. Hono, J. Appl. Phys. 100 (2006) 056105.
[13] T.O. Seki, Y.K. Takahashi, K. Hono, J. Appl. Phys. 103 (2008) 023910.
[14] T.J. Zhou, B.C. Lim, B. Liu, Appl. Phys. Lett. 94 (2009) 152505.
[15] Y.C. Wu, L.W. Wang, C.H. Lai, Appl. Phys. Lett. 93 (2008) 242501.
[16] J.L. Tsai, H.T. Tzeng, G.B. Lin, J. Alloy Compd. 487 (2009) 18–23.
[17] M. Fujikane, K. Kurosaki, H. Muta, S. Yamanaka, J. Alloy Compd. 393 (2005) 299–301.
[18] E. Lugscheider, K. Bobzin, M. MoÈller, Thin Solid Films 355 (1999) 367.
[19] J.S. Kim, Y.M. Koo, Thin Solid Films 516 (2008) 1147.